


MARCH 08 2024

Physics-based playability maps for single-reed woodwind instruments

Vasileios Chatziioannou  ; Montserrat Pàmies-Vilà; Alex Hofmann



JASA Express Lett. 4, 033201 (2024)

<https://doi.org/10.1121/10.0025281>





[LEARN MORE](#)

Advance your science and career as a member of the
Acoustical Society of America

Physics-based playability maps for single-reed woodwind instruments

Vasileios Chatziioannou,^{a)}  Montserrat Pàmies-Vilà, and Alex Hofmann
Department of Music Acoustics, University of Music and Performing Arts Vienna, Vienna, Austria
chatziioannou@mdw.ac.at, pamies-vila@mdw.ac.at, hofmann-alex@mdw.ac.at

Abstract: Musical instrument playability can be analyzed by visualizing a subspace defined by musicians' control parameters. This is common for bowed-string instruments in the form of Schelleng diagrams. Such diagrams can be populated either through experimental measurements or physical modeling. It was recently suggested to use similar diagrams for analyzing wind instrument playability. This study explores this direction using a physical model, previously validated against experimental measurements. It is shown that reed beating needs to be taken into account before playability analysis. This could help arrive at specific reed and mouthpiece designs according to the musicians' desires. © 2024 Author(s). All article content, except where otherwise noted, is licensed under a Creative Commons Attribution (CC BY) license (<http://creativecommons.org/licenses/by/4.0/>).

[Editor: D Murray Campbell]

<https://doi.org/10.1121/10.0025281>

Received: 24 January 2024 **Accepted:** 22 February 2024 **Published Online:** 8 March 2024

1. Introduction

Playability maps are often employed in music acoustics in order to analyze the function of the player-instrument system. Usually based on theoretical, heavily simplified physical models, they can help to predict the effect of certain control parameters on the system output. This allows to identify regions within a playability map where notes are easy or difficult to play, or where different regimes of oscillation are excited, subject to the control parameters. One such diagram that has attracted a lot of attention is the “Schelleng diagram” for bowed-string instruments (Schelleng, 1973). This depicts the area where the desired “Helmholtz motion” is achieved, subject to the input bow force and the position of the bow along the string, as depicted in Fig. 1. Musicians inherently learn how to stay within this playable wedge by fine-tuning the underlying control parameters (Schoonderwaldt, 2009).

While such diagrams may be drawn based on simplified analytical solutions, it is also possible to populate them either using experimental measurements or *via* physical modeling. It has been recently proposed by Woodhouse (2023) that similar diagrams could be obtained for different types of instruments. One such example was given for a single-reed woodwind instrument, considering the blowing pressure and the initial reed position (reed gap) as control parameters (see also euphonics.org, 2024) and depicting areas where a self-excited oscillation occurs. While the underlying physical models were of a simplified nature, Woodhouse (2023) proposes that “*extending the approach to more realistic models is a challenge for future research.*” Furthermore, a number of control parameters might be interesting to investigate, taking into account that the reed gap is affected by several factors, such as the geometry of the mouthpiece, the chosen reed, and the lip force within a range that is comfortable for the player.

In fact, for the case of the clarinet, physical modeling can now accurately predict the behavior of the player-instrument system for a wide variety of playing conditions (Chatziioannou *et al.*, 2019b). Synthesized waveforms have been shown to overlap with measured signals obtained under experimental conditions during both transient and steady-state regimes. This study presents playability diagrams for the clarinet, discussing the additional possibilities offered by the use of a more detailed physical model, with an enhanced set of control parameters.

2. The pressure-stiffness diagram

An experimental study on clarinet playability investigated sound characteristics subject to blowing pressure and lip force (Almeida *et al.*, 2013). Woodhouse (2023) recommended using the reed gap, instead of the lip force, as a control parameter, since it is a parameter that appears in most reed models. However, musicians adapt their lip force in order to allow sufficient reed gap in all dynamic levels (Brymer, 1976), thus attempting to maintain a constant reed gap. The model parameter that actually determines the required lip force, as controlled by the player, is the effective reed stiffness. Furthermore, the choice of “desirable” reeds is a problem that all players are familiar with, and this is directly related to

^{a)} Author to whom correspondence should be addressed.

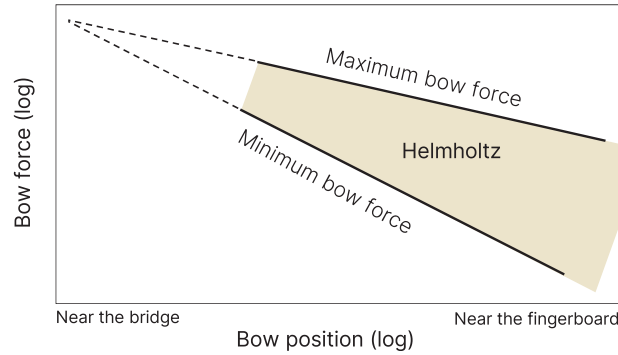


Fig. 1. Schelleng diagram sketch: Playing range of a bowed-string as a function of bow force and distance from the bridge to the bow. Based on Schelleng, J. Acoust. Soc. Am. 53(1), 26–41. (1973).

reed stiffness (usually referred to as “hardness” by manufacturers) (see Gangl *et al.*, 2016). Therefore, pressure-stiffness diagrams have been selected in this study for generating playability maps.

For an in-depth understanding of instrument behavior under player control, the model used in this study, outlined in Chatziioannou *et al.* (2019b), accurately handles viscothermal losses inside the tube and also takes reed beating into account. Embouchure effects due to the player’s tongue action are also modelled in order to simulate various articulation techniques. The performance of the model has been validated against experimental measurements using an artificial mouth (Mayer and Pàmies-Vilà, 2023), as well as against human performance (Chatziioannou *et al.*, 2019a). The equation that models the reed motion (displacement) y is

$$m \frac{d^2 y}{dt^2} + m\gamma \frac{dy}{dt} + ky + k_{\text{lay}} [y - y_{\text{lay}}]^{\alpha_{\text{lay}}} \left(1 + \eta_{\text{lay}} \frac{dy}{dt} \right) = S_r p_{\Delta}. \quad (1)$$

p_{Δ} is the pressure difference across the reed, with $p_{\Delta} = p_{\text{mouth}} - p_{\text{in}}$, where p_{in} is the pressure inside the mouthpiece and p_{mouth} is the blowing pressure; $m = 3.25$ mg is the effective reed mass, k is the effective reed stiffness, $\gamma = 3000$ s^{−1} is the reed damping, and $S_r = 98.6$ mm² is the effective reed surface. $k_{\text{lay}} = 1.97 \times 10^6$ N/m² is the collision stiffness for the reed–mouthpiece interaction (reed beating) and $[y]^{\alpha_{\text{lay}}} = \vartheta(y)y^{\alpha_{\text{lay}}}$, where $\vartheta(y)$ denotes the Heaviside step function and $\alpha_{\text{lay}} = 2$ is the collision exponent. $\eta_{\text{lay}} = 2$ s/m is the contact damping and $y_{\text{lay}} = 0.246$ mm is the mouthpiece height, indicating when contact begins. y_{lay} is smaller than the reed gap at rest ($y_{\text{eq}} = 0.41$ mm), since the reed–mouthpiece interaction begins before the reed is completely closed (Dalmont *et al.*, 2003).

The flow through the mouthpiece is composed by the Bernoulli flow u_f and the reed induced flow u_r as

$$u = u_f + u_r = \sigma \lambda (y_{\text{eq}} - y) \sqrt{\frac{2|p_{\Delta}|}{\rho}} + S_r \frac{dy}{dt}, \quad (2)$$

where $\sigma = \text{sign}(p_{\Delta})$, $\lambda = 1.2$ cm is the width of the reed, and ρ is the air density. A cylindrical tube of length $L = 0.4126$ m, without toneholes, is modelled using Webster’s equation, including viscothermal and radiation losses (Chatziioannou *et al.*, 2019b). Note, in particular, that the effective nature of the reed stiffness allows the model to encompass stiffness modifications due to both the player’s embouchure and the ligature.

Figure 2 shows a resulting pressure-stiffness diagram, generated using the above model, where combinations of the effective reed stiffness per unit area (k/S_r) and the blowing pressure (p_{mouth}) are tested. For each parameter set, the model is excited by a constant blowing pressure, with a linear attack of a 4 ms duration. Hence, the playability diagrams presented here correspond to a “cold start” (Woodhouse, 2023), where the acoustic pressure inside the tube is zero at time $t = 0$ and a sudden increase in the blowing pressure takes place. The result of the simulation for each parameter set is classified as unplayable if at least one of the following applies:

- the resulting mouthpiece pressure amplitude at steady state is lower than $\frac{1}{6}$ of the supplied blowing pressure;
- the fundamental frequency deviates more than 200 cent from the first resonance frequency of the tube. (It has been empirically identified that this only occurs when the reed “squeaks,” with the cent deviation being much larger.)

Note that: (i) reed stiffness increases downward, in order to get a similar orientation on the playability wedge as for Schelleng diagrams, (ii) contrary to Schelleng diagrams, the axes are scaled linearly, in accordance with the studies by Woodhouse (2023) and Almeida *et al.* (2023). A few observations can be made on the basis of this pressure-stiffness diagram. At first glance, it can be observed that in order to use a higher blowing pressure, players should choose a stiffer reed. This results in louder sounds without significantly affecting the spectral characteristics. In fact, the spectral centroid of the synthesized mouthpiece pressure (shown using the colorbar) may be kept constant if both blowing pressure and

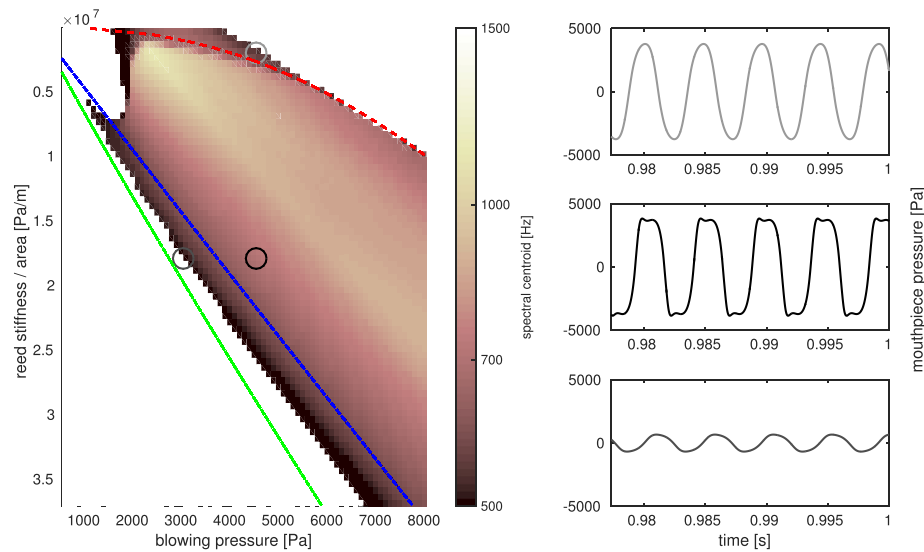


Fig. 2. Left: Pressure-stiffness diagram including theoretical threshold of oscillation (green), reed-beating threshold (blue), and saturation threshold (red). Right: Mouthpiece pressure at steady state for three selected case (circles in the pressure-stiffness diagram); from top to bottom: just above the saturation threshold; middle of the diagram; just above the oscillation threshold.

reed stiffness are increased simultaneously. It is also interesting to observe that at the edges of the wedged-shaped region, the spectral centroid is much lower, indicating that a tone lacking harmonic components is produced, sometimes referred to by musicians as *subtone*. This is in accordance with the playability thresholds shown in the diagram, as calculated in [Dalmont and Frappé \(2007\)](#). Namely, the green line at the left of the wedge is the oscillation threshold, below which, according to a simplified theoretical reed model, reed oscillations are not possible from a cold start. This is indeed the case for the numerically generated diagram. The blue line crossing through the wedge corresponds to the reed-beating threshold. Above this line, the blowing pressure is sufficient for reed beating to take place, resulting in an overtone-rich spectrum. This is also in agreement with the diagram, since the spectral centroid increases above this line. Finally, the red line at the top of the wedge is the saturation threshold, above which the resulting mouthpiece pressure stops increasing for an increasing blowing pressure, until oscillations completely vanish after further increase in the blowing pressure. This line marks another transition within the playability wedge between areas with a high spectral centroid and areas with a lower one.

These cases are exemplified on the right-hand-side plots in Fig. 2 by showing steady-state waveforms at three different diagram locations:

- *Bottom plot:* Playing conditions just above the oscillation threshold. This results in a mouthpiece pressure of much lower amplitude (673 Pa) than the supplied blowing pressure (3000 Pa) and with the energy mostly contained at the fundamental frequency.
- *Middle plot:* Playing conditions above the beating threshold (this is the most commonly played region) where a typical clarinet-like signal is obtained. The same reed stiffness as above is used, with a higher blowing pressure. The amplitude of the mouthpiece pressure (3820 Pa) is much closer to the supplied pressure (4500 Pa).
- *Top plot:* Playing conditions just above the saturation threshold. The same blowing pressure as above is used (4500 Pa) with a higher reed stiffness. The amplitude of the mouthpiece pressure remains high (3770 Pa) but the spectral centroid is much lower, with the waveform becoming less like a square-wave.

2.1 Varying reed beating parameters

A question that remains to be addressed is how variation in other model parameters may affect the playability characteristics highlighted by such diagrams. In this study, we focus on the collision model parameters, namely the collision stiffness k_{lay} and the collision exponent α_{lay} . The former may be roughly associated with the “hardness” of the collision, thus depending on the material properties of the reed and the mouthpiece. The latter reflects the way the reed curls upon the mouthpiece lay ([Chatziioannou and van Walstijn, 2012](#); [Dalmont et al., 2003](#)) and therefore depends on the geometry of the mouthpiece, but also on the position of the player’s lower lip. By keeping the reed stiffness constant and varying the above two parameters, different playability diagrams may be obtained, as shown in Fig. 3. It can be observed that an increasing collision stiffness (left), or a decreasing collision exponent (right), both result in a higher blowing pressure being necessary to initiate oscillations. Note that a decreasing collision exponent corresponds to a more drastic collision.

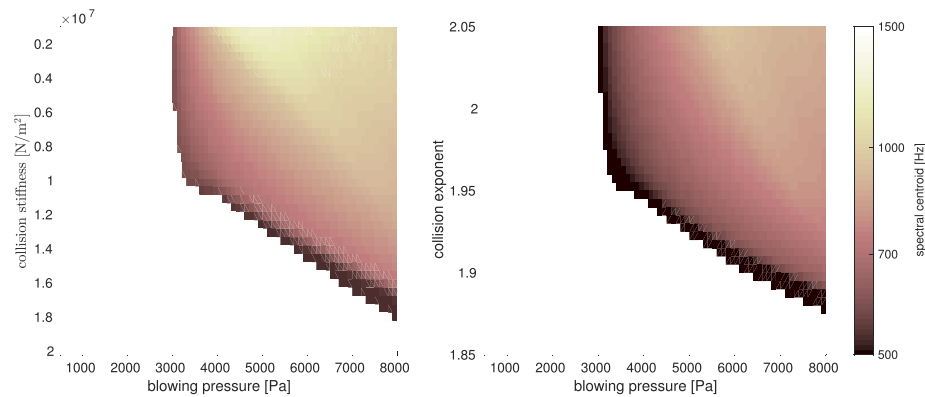


Fig. 3. Left: Pressure-collision stiffness diagram for a constant reed stiffness $k = 1.79 \times 10^7$ N/m and $\alpha_{lay} = 2$. Right: Pressure-collision exponent diagram for the same reed stiffness and $k_{lay} = 1.97 \times 10^6$ N/m².

Therefore, only the collision stiffness increases downward in these plots, in accordance with the reed stiffness in Fig. 2. The spectral characteristics, as indicated by the spectral centroid, also vary subject to parameter variation. This is in line with the findings by Gazengel *et al.* (2016) that the reed–mouthpiece interaction during playing should not be ignored. Thus, when attempting to draw conclusions regarding instrument playability from physical models, one should aim to include as many acoustically significant effects as possible. While this may pose additional obstacles toward theoretical analyses, it allows us to better understand the function of the player–instrument system.

The above observations indicate that considering variations in only two parameters may be a restrictive factor for analyzing the playability of some instruments. While two-dimensional diagrams are easier to obtain and interpret, additional dimensions may yield fruitful insights on playability. One such example is shown in Fig. 4 where several layers of a pressure–stiffness diagram are plotted for slightly different collision exponent values (α_{lay}). It can be observed how the playability characteristics significantly vary for small changes in α_{lay} . The small “non-playable” gap that appeared in the top left corner of Fig. 2 seems to propagate towards the middle of the playability wedge for a decreasing α_{lay} . It has been verified that this gap appears, regardless of the chosen playability criteria, with no self-sustained oscillations being achieved in this region. Furthermore, subtones are generated for a much larger area within the wedge in the case of lower α_{lay} . The saturation threshold still coincides with regions of different spectral characteristics, as evident by the color change across it. Figure 4 suggests that reed beating, as well as variations in the related parameters, need to be considered when addressing playability in single-reed woodwind instruments. These findings may also be relevant for other wind instruments involving collisions (e.g., double-reed, lip, or vocal-fold collisions).

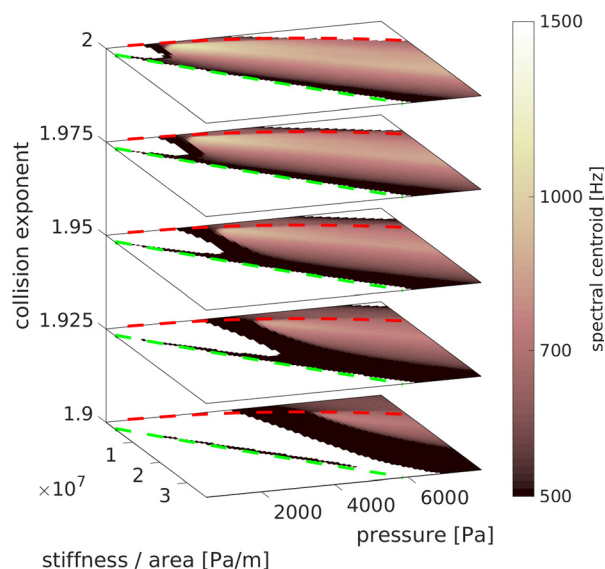


Fig. 4. Pressure-stiffness diagrams for different values of the collision exponent α_{lay} , including the oscillation (green) and saturation (red) thresholds.

3. Discussion

Acquiring a high quality sound with single-reed woodwind instruments, like clarinet or saxophone, requires both years of practice and suitable equipment. This especially involves choosing the right combination of mouthpiece and reed to generate the desired sound within a comfortable playing regime of blowing pressure and lip pressure. The search for the right equipment is often time-consuming and costly, as players have a large range of different product combinations from which to choose, and then have to test these out in different playing scenarios. Depending on the musical requirements, different equipment is needed. For example, performing in a classical Viennese chamber music ensemble requires different equipment (hard reed, mouthpiece with small tip opening) compared to a clarinet soloist in a jazz big band who needs equipment (softer reeds, larger tip opening) to be as loud or louder than the rhythm section and brass instruments. Recommendations by teachers, colleagues, or copies of established equipment help performers to navigate this vast landscape of choices; however, the component of individual playing comfort is not guaranteed.

The presented approach suggests that a physics-based analysis of equipment and required performance parameters could help predict the resulting sound. This may inform musicians in a comparable and orderly fashion about certain reed–mouthpiece combinations, their impact on playing comfort (required blowing pressure) and the expected outcome. In order to provide such detailed information, further research on material properties, interactions between different material types, and the effect of various mouthpiece geometries is required. Information obtained using physical modeling, prior to manufacturing stages, may allow designing specifically targeted synthetic reed–mouthpiece combinations for certain player requirements.

Acknowledgments

This research was funded in whole or in part by the Austrian Science Fund (FWF) [10.55776/(P34852, T1295, and AR743)].

Author Declarations

Conflict of Interest

The authors have no conflicts to disclose.

Data Availability

The data that support the findings of this study are available from the corresponding author upon reasonable request.

References

- Almeida, A., George, D., Smith, J., and Wolfe, J. (2013). "The clarinet: How blowing pressure, lip force, lip position and reed 'hardness' affect pitch, sound level, and spectrum," *J. Acoust. Soc. Am.* **134**(3), 2247–2255.
- Brymer, J. (1976). *Clarinet* (Macmillan, New York).
- Chatziioannou, V., Schmutzhard, S., Hofmann, A., and Pàmies-Vilà, M. (2019a). "Inverse modelling of clarinet performance," in *Proceedings of the International Congress on Sound and Vibration*, Montreal (International Institute of Acoustics & Vibration, Auburn, AL), pp. 4822–4828.
- Chatziioannou, V., Schmutzhard, S., Pàmies-Vilà, M., and Hofmann, A. (2019b). "Investigating clarinet articulation using a physical model and an artificial blowing machine," *Acta Acust. united Acust.* **105**(4), 682–694.
- Chatziioannou, V., and van Walstijn, M. (2012). "Estimation of clarinet reed parameters by inverse modelling," *Acta Acust. united Acust.* **98**(4), 629–639.
- Dalmont, J., and Frappé, C. (2007). "Oscillation and extinction thresholds of the clarinet: Comparison of analytical results and experiments," *J. Acoust. Soc. Am.* **122**, 1173–1179.
- Dalmont, J., Gilbert, J., and Ollivier, S. (2003). "Nonlinear characteristics of single-reed instruments: Quasistatic volume flow and reed opening measurements," *J. Acoust. Soc. Am.* **114**(4), 2253–2262.
- euphonics.org (2024). "Euphonics: The science of musical instruments," Chap. 11, available at <https://euphonics.org/> (Last viewed February 15, 2024).
- Gangl, M., Hofmann, A., and Mayer, A. (2016). "Comparison of characterization methods for B-flat clarinet reeds," in *7th Alps Adria Acoustics Association Congress on Sound and Vibration* (Slovenian Acoustical Society, Ljubljana, Slovenia), pp. 179–186.
- Gazengel, B., Dalmont, J., and Petiot, J. (2016). "Link between objective and subjective characterizations of Bb clarinet reeds," *Appl. Acoust.* **106**, 155–166.
- Mayer, A., and Pàmies-Vilà, M. (2023). A blowing and tonguing device for artificial excitation of single-reed woodwind instruments (RIAM 2.0–Reed Instrument Artificial Mouth Technical Report), available at <https://doi.org/10.21939/iwk-tech-report-1-2023>.
- Schelleng, J. (1973). "The bowed string and the player," *J. Acoust. Soc. Am.* **53**(1), 26–41.
- Schoonderwaldt, E. (2009). "The player and the bowed string: Coordination of bowing parameters in violin and viola performance," *J. Acoust. Soc. Am.* **126**(5), 2709–2720.
- Woodhouse, J. (2023). "Mapping playability: The Schelleng diagram and its relatives for bowed strings and wind instruments," in *Stockholm Music Acoustics Conference 2023*, edited by S. D'Amario, S. Ternström, and A. Friberg Stockholm, Sweden, pp. 1–8.